Pharm Res (2013) 30:2917–2930
DOI 10.1007/s11095-013-1123-3

RESEARCH PAPER

The Use of Condensational Growth Methods for Efficient Drug Delivery to the Lungs during Noninvasive Ventilation High Flow Therapy

Laleh Golshahi • Geng Tian • Mandana Azimi • Yoen-Ju Son • Ross Walenga • P. Worth Longest • Michael Hindle

Received: 27 March 2013 / Accepted: 11 June 2013 / Published online: 26 June 2013

ABSTRACT

Purpose The objective of this study was to evaluate the delivery of nasally administered aerosols to the lungs during noninvasive ventilation using controlled condensational growth techniques.

Methods An optimized mixer, combined with a mesh nebulizer, was used to generate submicrometer aerosol particles using drug alone (albuterol sulfate) and with mannitol or sodium chloride added as hygroscopic excipients. The deposition and growth of these particles were evaluated in an adult nose-mouth-throat (NMT) model using *in vitro* experimental methods and computational fluid dynamics simulations.

Results Significant improvement in the lung dose (3–4× increase) was observed using excipient enhanced growth (EEG) and enhanced condensational growth (ECG) delivery modes compared to control studies performed with a conventional size aerosol (~5 μm). This was due to reduced device retention and minimal deposition in the NMT airways. Increased condensational growth of the initially submicrometer particles was observed using the ECG mode and in the presence of hygroscopic excipients. CFD predictions for regional drug deposition and aerosol size increase were in good agreement with the observed experimental results.

Conclusions These controlled condensational growth techniques for the delivery of submicrometer aerosols were found to be highly efficient methods for delivering nasally-administered drugs to the lungs.

KEY WORDS combination drug-excipient particles · enhanced condensational growth · excipient enhanced growth · hygroscopic growth · noninvasive aerosol therapy · nose-to-lung aerosol delivery

ABBREVIATIONS

ACI	Andersen cascade impactor
AS	albuterol sulfate
CFD	computational fluid dynamics
DF	deposition fraction
ECG	enhanced condensational growth
EEG	excipient enhanced growth
GSD	geometric standard deviation
HFT	high flow therapy
HPLC	high performance liquid chromatography
LRN	low Reynolds number
MMAD	mass median aerodynamic diameter
MN	mannitol
NaCl	sodium chloride
NIV	noninvasive ventilation
NMT	nose-mouth-throat model
NPPV	noninvasive positive pressure ventilation
RH	relative humidity
SD	standard deviation

INTRODUCTION

Noninvasive ventilation (NIV) is a preferred method, compared to invasive methods such as endotracheal intubation, for long-term and ambulatory gas delivery in patients with chronic respiratory diseases and to improve breathing in patients with sleep apnea (1). The popularity of the NIV technique is due to its convenience, safety and low cost (2). Current NIV methods include noninvasive positive pressure ventilation (NPPV) (3) and high flow therapy (HFT). The

L. Golshahi (✉) • M. Azimi • Y.-J. Son • P. W. Longest • M. Hindle
Department of Pharmaceutics
Virginia Commonwealth University
410 N 12th St., Box 980533, Richmond, Virginia, USA
e-mail: lgolshahi@vcu.edu

G. Tian • R. Walenga • P. W. Longest
Department of Mechanical and Nuclear Engineering
Virginia Commonwealth University
Richmond, Virginia, USA

advent of HFT for continuous flow delivery, in which preconditioned (heated and humidified) air or blended oxygen is delivered *via* a nasal cannula, has allowed higher delivered flow rates (from 5 to 45 L/min) to patients ranging in age from preterm newborns to adults (4).

Patients who receive NIV are also typically prescribed pharmaceutical aerosols for treatment of their respiratory health issues (5). Although aerosol drug delivery during NIV *via* nasal cannula is an attractive method, long nebulization times of high doses and frequent administration of short-acting drugs are needed (6). These NIV inhalation therapies have shown poor lung delivery efficiencies, which are on the order of 1–10% for adults (3) and children (7) *in vitro* and 1–6% for adults (8) *in vivo*. Aerosol losses are mostly due to high deposition in the ventilation circuit and nasal passages. The heated and humidified gases that are used during HFT are also considered as contributing components that intensify the losses in ventilation lines and cannulas (9). Bench models have shown a reduction of up to 40% in aerosol delivery in heated and humidified ventilation circuits compared to unheated and non-humidified systems (10,11). Such high losses result in a large amount of drug waste and highly variable delivered dose; thus, aerosol delivery during HFT is not currently favored, especially for treatments with expensive drugs or formulations with a narrow therapeutic index.

Efforts have been made to improve inhalation drug delivery during NIV, which are summarized in recent reviews (2,5). However, despite advancements in ventilator and device designs, significant aerosol losses still occur in the ventilation circuit and the nasal airways of the patients (2).

In order to improve drug delivery to the lungs during HFT, a novel concept of aerosol delivery through nasal airways using enhanced condensational growth (ECG) has recently been proposed by Longest *et al.* (12). In their study, which demonstrated low drug deposition in a physically realistic nose and upper airway model, submicrometer particles (mass median aerodynamic diameter (MMAD) = 900 nm) of albuterol sulfate (AS) were generated using a commercial small particle aerosol generator and delivered at 10 L/min and 21°C to one nostril at subsaturated conditions, whereas heated and humidified air was delivered at 20 L/min and 39°C through the other nostril. The submicrometer particles had minimal deposition within the nasal and upper airway model. With ECG delivery, aerosol deposition in the nose was 14.8% of the dose compared to 72.6% for a 4.7 μm aerosol. The nasal septum separated the two airstreams and prevented hygroscopic growth until the streams were combined as they entered the nasopharynx. Combination of these streams resulted in supersaturation and produced an increase in aerosol size to about 1.9 μm as the aerosol exited the trachea, which would enable deposition of the aerosol within the lung and prevent exhalation. Despite the success of Longest *et al.* (12) in producing a significant reduction of losses using the ECG nose to lung delivery method, the study was limited due to the nebulizer employed and the lack of a realistic patient cannula. In order to address these shortcomings, Longest *et al.* (13) developed a novel submicrometer aerosol generation system that facilitates the use of conventional low volume-fill medical nebulizers by drying the generated droplets in an efficient mixer (*i.e.* with minimal losses), and heating the aerosol (~ 37°C) at a desired flow rate (*e.g.* 15–30 L/min) to achieve suitable patient comfort (13). Furthermore, they designed streamlined cannulas, which minimize drug deposition during inhalation (13,14). The suitability of the new generation system and the streamlined cannulas in lowering deposition in the nose and improving the aerosol lung delivery will be evaluated in this study.

The condensational growth technique has been shown *in vitro* to significantly improve the lung delivery of nasally-administered drugs during HFT. However, there are situations where the addition of heated and humidified air to produce airway supersaturation is not feasible, for instance during NPPV. Hindle and Longest (15–17) proposed the use of various hygroscopic excipients at different drug:excipient ratios which would produce growth of submicrometer particles in the natural humidity of the lungs. This inhaled drug delivery concept, which is known as excipient enhanced growth (EEG), was demonstrated *in vitro* using a mouth-throat-tracheobronchial model (18,19). Oropharyngeal drug deposition was shown to be low (<1%) for an albuterol sulfate:mannitol (0.4%:0.4% w/v) formulation with an initial MMAD of 0.47 μm, which grew to 1.66 μm at the exit of the model (18). Numerical simulations have demonstrated the possibility of the further growth of the submicrometer particles, without increasing the extrathoracic deposition, by increasing the initial particle size to a value closer to 900 nm (17–19). This specific particle size provides a good balance between low extrathoracic deposition and high drug payload delivery (13,16,18).

The EEG technique has been demonstrated for orally inhaled drug delivery (18,19) and ECG has been demonstrated for both oral (20) and nasal (12) inhalation with excellent results. The current study seeks to investigate the application of EEG delivery of nasally administered submicrometer combination aerosols using the newly designed streamlined cannula (14) as the delivery interface and the new submicrometer aerosol mixer generation system (13), with different formulations. For EEG aerosol delivery, the mixer system provides a steady flow rate of 30 LPM, which can be applied as a single unit device for nose-to-lung aerosol administration or for concurrent HFT with aerosol drug delivery. The concept of ECG aerosol delivery will also be explored in which a divided cannula (13) is used to deliver the submicrometer aerosol from the mixer to one nostril and standard HFT from a commercial device is applied to the other nostril. In the ECG application, drug only aerosols are considered in addition to formulations containing drug and hygroscopic excipients. As a result, the current study extends the development of controlled condensational growth

techniques (EEG and ECG) for nasally administered aerosols using a high efficiency source of aerosol production, newly designed streamlined cannulas, and new formulation combinations. Drug delivery to the lungs is assessed using both *in vitro* experiments and CFD simulations within an airway model of the nose and throat extending through the trachea.

MATERIALS AND METHODS

Formulations for Excipient Enhanced Growth Experiments

For EEG studies, two formulations were investigated containing a 50:50 drug:excipient ratio to study the effect of hygroscopic excipient type on aerosol deposition and growth. The two formulations were (i) 0.2% albuterol sulfate (AS): 0.2% mannitol (MN) and (ii) 0.2% AS:0.2% sodium chloride (NaCl) w/v in deionized water. Solutions were prepared freshly each day and stored at room temperature prior to use. The formulations were stable at room temperature during this time period, however an extended evaluation of stability was beyond the scope of this study. The hygroscopic parameters, which describe the hygroscopic growth potential of a soluble compound, are 4.9 for AS, 8.2 for MN, and 77.9 kmol/m^3 for NaCl (16) with the larger values representing the more hygroscopic material. These values imply that NaCl and AS are, respectively, the most and the least hygroscopic constituents of the formulations among all three components with MN having an intermediate value.

Formulations for Enhanced Condensational Growth Experiments

For the ECG studies, three formulations were investigated containing drug only and 50:50 drug:excipient formulations (NaCl and MN). The three formulations were (i) 0.2% AS, (ii) 0.2% AS: 0.2% MN, and (iii) 0.2% AS: 0.2% NaCl w/v in deionized water. Solutions were prepared freshly each day and stored at room temperature prior to use. The formulations were stable at room temperature during this time period.

Aerosol Generation and Characterization

Submicrometer particles from the EEG and ECG formulations were generated using the improved mixer system proposed by Longest *et al.* (13) in combination with the Aeroneb Lab nebulizer (Aerogen Limited, Ireland). The Aeroneb Lab nebulizer has a reported nominal droplet volume median diameter of 2.5–4.0 μm. In brief, the Aeroneb Lab mesh nebulizer containing the test formulation was inserted into the nebulizer inlet on the mixing chamber and compressed air at the flow rate of 15 LPM (ECG) or 30 LPM (EEG) was supplied to the mixer air inlet (Fig. 1a). The air was heated by the internal Kapton heaters (OMEGALUX KHLV-202; Omega Engineering Inc., Stamford, CT) to a temperature in the range of 37 ± 2°C prior to combining with the nebulizer aerosol output. The heated air mixes with the liquid aerosol droplets from the nebulizer in the drying region, the result of which is the evaporation of the droplets and the formation of submicrometer-sized particles, which are delivered to the *in vitro* airway model. The nebulization duration was 0.5 min for both the ECG and EEG studies.

Control experiments were performed to observe differences in the drug deposition characteristics using the Aeroneb nebulizer to produce conventional sized aerosols. In these control experiments as shown in Fig. 1a, the nebulizer was placed in the Aeroneb neonatal T-adapter (Aerogen Limited, Ireland), and aerosol was delivered to the *in vitro* airway model using a commercial HFT unit (Vapotherm 2000i, Stevensville, USA), which was used to generate flows of 15 LPM (ECG) or 30 L/min (EEG). The humidified air from the Vapotherm (RH >90%) prevented evaporation of the aerosol droplets during transit through the ventilator tubing and cannula. Due to lower drug delivery to the impactor in these studies, the nebulization duration was extended to one minute. For comparison with EEG delivery, control studies were performed using formulations of 0.1% AS: 0.1% MN and 0.1% AS:0.1% NaCl w/v in deionized water. For the comparison with ECG delivery, a control study was performed using a 0.2% AS w/v in deionized water. The size of the aerosol exiting the cannula was measured by positioning the cannula at the inlet of the ACI operating at 30 LPM, which was placed in the environmental chamber (25 ± 0.5°C, RH > 90%). In the ECG protocol, an additional 15 LPM was drawn through the humidity inlet of the ECG cannula from the cabinet.

The initial aerodynamic particle size distribution of the drug aerosol leaving the mixer and also in the absence of the mixer (control) was measured for comparison with the size of aerosol exiting the NMT model to quantify the aerosol growth during inhalation. This initial size measurement was carried out by connecting the mixer's outlet (EEG and ECG submicrometer particle generation) to the Andersen Cascade Impactor (ACI, Copley Scientific, UK) using ventilation tubing (50 cm length, I.D. = 10 mm). The ACI was placed in an environmental cabinet (Espec; Hudsonville, MI) with internal conditions of 37 ± 0.5°C and RH > 90%. An impactor flow rate of 30 LPM was employed for particle sizing. For the ECG study, an additional 15 LPM of heated and humidified air was supplied to the impactor from the environmental cabinet to maintain isothermal conditions during sizing. No additional air was required for the EEG studies which operated at 30 LPM.

Similar studies were performed for the control experiments to determine the initial size of the aerosol emitted from the Aeroneb in the absence of the mixer by positioning the nebulizer

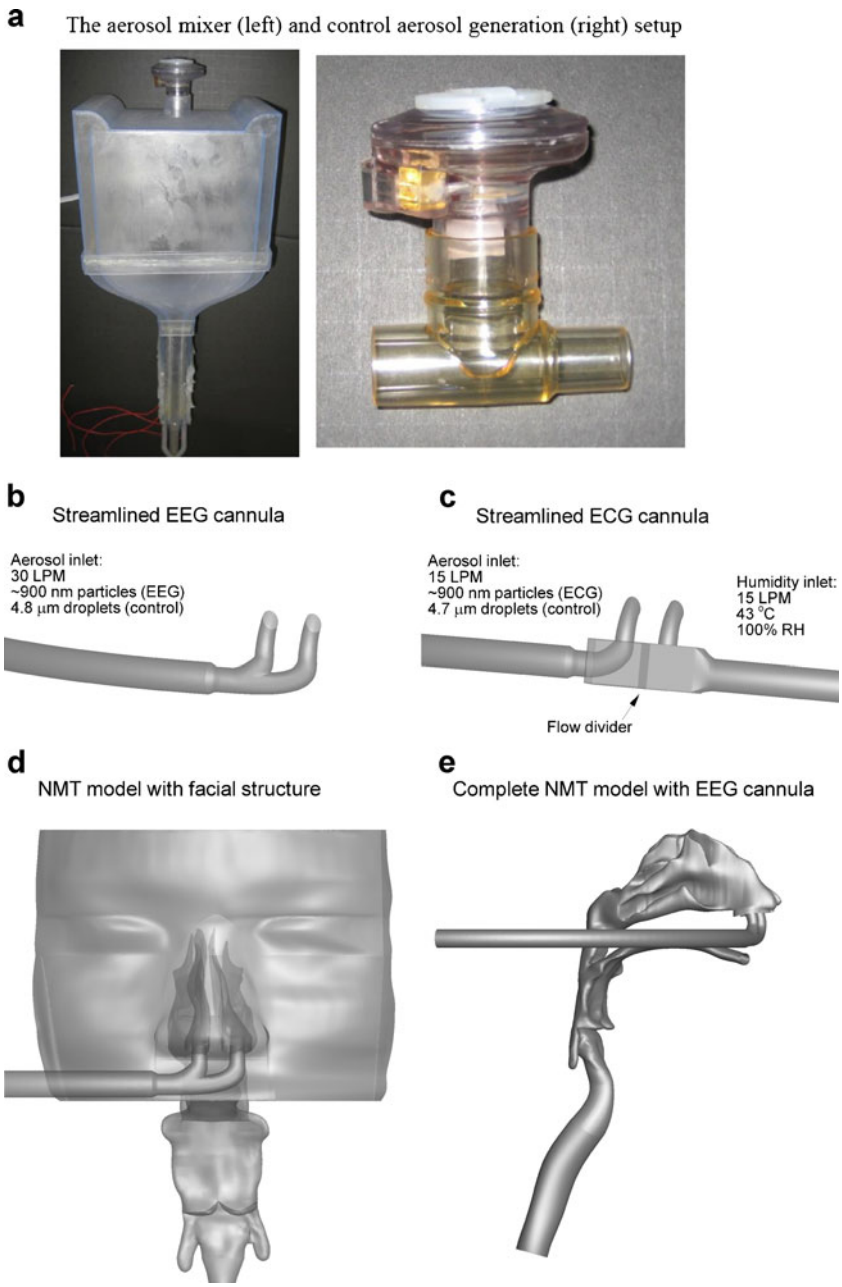

Fig. 1 The experimental and numerical systems for evaluating controlled condensational growth including (**a**) the aerosol mixer (*left*) and control aerosol generation (*right*) setups, (**b**) the EEG delivery streamlined cannula interface, (**c**) the divided and streamlined ECG delivery cannula, (**d**) the nose-mouth-throat (NMT) model including the external face structure with the EEG cannula positioned in the nostrils, and (**e**) the complete NMT model with EEG cannula.

directly over the ACI inlet, which was placed in the environmental chamber (25 ± 0.5°C, RH > 90%) with an approximate gap distance of 10 mm to allow for air entrainment.

In Vitro Model Setup for EEG and ECG Aerosol Delivery

Aerosol exiting the mixer is delivered to an *in vitro* airway model as shown in Fig. 1d. A 50 cm length of 10 mm internal diameter ventilator tubing (Instrumentation Industries Inc., USA) was attached to the exit of the mixer. This was connected to the cannula setup consisting of a 20 cm length of 10 mm internal diameter ventilator tubing (Instrumentation Industries Inc., USA) and a streamlined designed cannula. The EEG cannula consisted of a streamlined single inlet cannula as described by Longest *et al.*(14), which divides the incoming flow into two separate streams for the two nasal inlets using smooth curvatures (Fig. 1b). Such smooth curvatures reduce the losses that normally occur in conventional cannulas due to sudden changes of flow direction. The EEG cannula was employed with aerosol delivered from the mixer at 30 LPM. The divided ECG cannula, which was described by Longest *et al.* (13), had separate inlets for aerosol from the mixer flowing at 15 LPM and for heated/humidified air at 15 L/min (Fig. 1c). Similarly, the aerosol path was streamlined (using smoothed curvatures) to minimize depositional drug losses. The ECG cannula was

employed with aerosol delivered from the mixer at 15 LPM to the aerosol inlet of the cannula and 15 LPM of heated (43°C) and saturated air from the HFT unit (Vapotherm 2000i) to the cannula air inlet. The air inlet was left open to cabinet conditions for the control experiment in order to not produce ECG growth conditions.

The cannula was inserted into the nostrils of a physically realistic nose-mouth-throat (NMT) *in vitro* model. The realistic airway model consisted of an external facial structure for connecting the cannula, the nasal passages, nasopharynx, a portion of the mouth, pharynx, larynx, and trachea (Fig. 1d and e). A single high quality medical scan was not available containing all of these features. Instead, several scans were selected to develop a characteristic model based on healthy adult males with an age range of 34–54 years. The nasal geometry is based on the frequently employed dataset of Guilmette (1989) (21), which has been used in previous *in vitro* (12,22,23) and CFD studies (12,24,25). The multi-slice images were segmented in MIMICS (Materialize, Ann Arbor MI) according to the tissue-air contrast and were converted into a set of coronal polylines that defined the nasal airway. Based on these contours, an internal nasal surface geometry was constructed in Gambit 2.3 (ANSYS Inc., Canonsburg, PA). As with previous studies, the nasal data set was smoothed to produce a physiologically realistic 3D structure. Following the same procedure, an external nasal structure and the airways below the nasal passages were constructed from characteristic CT scans of adults. In the final NMT model, the hydraulic diameter of the glottis was 9.8 mm, which is consistent with previous studies (26). Similarly, the tracheal hydraulic diameter was 18.7 mm, which was determined to be consistent with the mean value of an internal database of CT scans. The model ended at the position where the trachea begins to expand and form the first bifurcation.

The airway geometry was constructed for the *in vitro* experiments using in-house rapid prototyping facilities. A Viper SLA machine (3D Systems, Valencia, CA) constructed an exact replica of the airway geometry out of clear Accura 60 plastic resin using a build layer thickness of 0.15 mm and a laser spot diameter of 0.25 mm. The outlet of the NMT *in vitro* model was connected directly to an ACI for aerosol sizing at an airflow rate of 30 LPM. The walls of the model were prewetted and the model, together with the impactor, was housed in an environmental cabinet (Espec; Hudsonville, MI) to maintain a wall temperature of approximately 37 ± 0.5°C and relative humidity of 99%.

Data Analysis

The concentration of the drug (albuterol sulfate, AS) in each formulation was determined by a previously validated high performance liquid chromatography (HPLC) analytical method (27). Before and after each experiment, the nebulizer was weighed and the weight difference, together with the concentration of albuterol sulfate in the formulation, was used to calculate the nominal dose. After each experiment, the nebulizer, 50 and 20 cm ventilator tubing, cannula, *in vitro* airway model, and the impactor stages of the ACI were washed with deionized water. Wash volumes were 10 ml for each deposition location in the setup, except for the nose and the filter stage of the ACI that were washed with 20 ml of water to either keep the concentration of the drug within the HPLC calibration curve or to have enough volume to cover the deposition surface. The AS concentrations of the solutions collected from each site of deposition were determined using HPLC and were used together with the wash volumes to calculate the deposited AS mass. The total recovered mass was used to calculate the percentage of deposition at each deposition site as a fraction of the nominal dose. Cumulative distribution of the deposited mass on each stage of the ACI was used to calculate the mass median aerodynamic diameter (MMAD) and geometric standard deviation (GSD) for each experimental condition. Three to five replicates of each experimental configuration were performed for each case study. One-way ANOVA, followed by a *post hoc* Tukey's Honest Significance Difference (HSD) test, (JMP 9, Cary NC) was used for statistical analysis with a p-value of <0.05 indicating significance.

CFD Simulations

The CFD simulations performed were similar to the previous nasal ECG (12) and oral EEG (18) studies and employed the Fluent 12 (ANSYS Inc.) software supplemented with user routines. In brief, a low Reynolds number (LRN) k-ω turbulence model was used to simulate the flow, which can be laminar, transitional, or turbulent at different locations in the flow field. This turbulence model has previously been used for the successful prediction of aerosol transport and deposition in upper airway models (26,28,29). To evaluate the variable temperature and relative humidity fields, the coupled governing equations of heat and mass transport, reported in detail by Longest and Xi (30) and Longest *et al.* (31), were used. Lagrangian transport equations coupled with user-defined functions were employed to estimate the particle trajectories, growth, and deposition. User-defined functions were implemented to improve estimation of near-wall conditions and to simulate the aerosol evaporation and condensation in the complex three-dimensional temperature and humidity fields (12). User-defined functions were also used to account for anisotropic near-wall turbulent dispersion, Brownian diffusion of the initially submicrometer aerosols, and near-wall interpolation of fluid velocities (12). Our previous studies have demonstrated that this combination of a commercial code with multiple user-defined functions is capable of accurately capturing particle deposition arising from inertia, sedimentation, diffusion, and turbulent dispersion

(19,31). The Kelvin effect, influences of excipient and drug hygroscopicity, and the effect of droplet temperature on surface vapor pressure were considered in the droplet size change calculations based on previous studies (12). The influence of the droplet on the carrier phase was neglected and a one-way coupled approach was implemented in the model. The details of solving the above equations using realistic boundary conditions can be found in Longest *et al.* (12) and Tian *et al.* (18).

For simulating droplet trajectories and aerosol size increase, initially monodisperse size distributions were implemented. Condensational growth of the aerosols then led to a polydisperse aerosol size distribution within the airway models. With the control experiments, an initial droplet size of 3.6 μm was found to match the experimentally measured aerosol size exiting the nasal cannula and entering the NMT model. The aerosol size exiting the Aeroneb Lab nebulizer could not be implemented directly due to high depositional losses in the neonatal T-connector, which reduced the MMAD of the aerosol and was not included in the CFD model. For the EEG and ECG simulations, the experimentally measured size exiting the mixer tubing (900 nm) was implemented at the model inlet. In all droplet simulations, 9000 initial particles were injected into the steady state flow stream and increasing this number had a negligible effect on deposition fractions.

The computational mesh was constructed using the ANSYS ICEM 10 package (Ansys Inc., Canonsburg, PA) and consisted of tetrahedral and hexahedral elements. Hexahedral control volumes were used primarily in the connective tubing, cannula geometry, and tracheal region, whereas tetrahedral elements with a thin layer of near-wall wedge control volumes were used to resolve the nasal passages through the pharynx. Grid density testing produced convergent results in terms of regional deposition for a control volume cell count of approximately 1.3 million for the EEG NMT geometry and 1.5 million for the ECG NMT model.

RESULTS

Characterization of Delivered Aerosols

For the EEG setup with 30 LPM drying air, the mean (SD) MMAD of the aerosol exiting the mixer system for the 0.2% AS:0.2% NaCl formulation was 0.91 (0.05) μm. The mean (SD) geometric standard deviation (GSD) was 2.11 (0.08) μm. Similar mean (SD) MMADs were observed for both the 0.2% AS formulation (0.88 (0.02) μm) and the 0.2% AS:0.2% NaCl formulation (0.91 (0.08) μm) using the ECG setup with a flow rate of 15 LPM through the mixer. The respective GSDs were 1.91 (0.02) and 2.09 (0.12). These results confirm the previous findings that the improved mixer is capable of producing submicrometer aerosols with a mean size around 0.9 μm suitable for the condensational growth applications (13).

For the control experiments, which were designed to examine the aerosol deposition characteristics of a conventional sized aerosol during HFT, the mean (SD) MMAD for the 0.1% AS:0.1% NaCl formulation was 4.77 (0.07) μm. The mean (SD) GSD of this polydisperse aerosol was 3.94 (0.69). The MMAD of the aerosol exiting the EEG cannula was reduced to 2.9 (0.3) μm with the mean (SD) GSD of 1.6 (0.09). The mean (SD) for the 0.2% AS formulation was 4.66 (0.03) μm with a GSD of 2.19 (0.45). The MMAD of the aerosol at the exit of the ECG cannula was 3.4 (0.25) μm with the mean (SD) GSD of 1.7 (0.15).

EEG *In Vitro* Deposition

Table I shows the mean (SD) deposition fraction of AS on the delivery device components following aerosolization and delivery to the *in vitro* airway model for the EEG protocol and its control experiments. Drug deposition on the Aeroneb Lab nebulizer was low (<3%) in the control experiments and the EEG experiments, however there was a significant difference observed between the EEG aerosols and their respective controls ($p=0.0332$ with MN and $p=0.0013$ with NaCl). The Aeroneb T-connector was a significant site of drug deposition in the control experiments as the micrometer sized aerosol impacts on this device during mixing with the HFT air. Comparing deposition in the 50 cm ventilator tubing that delivers the aerosol from the mixer or T-connector, respectively, there was significantly higher deposition for the micrometer sized aerosols in the control experiments compared to the submicrometer aerosol generated in the EEG experiments for both test formulations ($p<0.0001$). There was no significant difference between deposition in the 20 cm ventilator tubing for the AS:MN EEG formulation compared to the control experiments ($p=0.8$), but deposition in this device component was significantly lower for the AS:NaCl formulation compared to the control experiments ($p=0.002$). Deposition within the streamlined EEG cannula was about 0.5% of the nominal dose for the submicrometer EEG formulations compared to about 13% for the control experiments, which indicated that decreasing the size of aerosol significantly lowers the deposition in the cannula ($p<0.0001$ with both excipients). Previous studies have indicated that deposition in the mixer was low (about 8% of the nominal dose), with this estimate being based upon the difference between the nominal dose and the total recovered dose (13). Similar estimates for mixer deposition for the AS:MN and AS:NaCl formulations were 13.3 and 5.6%, respectively. These estimates are conservatively high and likely over predict the losses in the mixer due to the more complicated experimental setup employed and the number of washing steps required to recover the drug in this study.

Figure 2 shows the % deposition of AS in the complete delivery device (T-connector or estimated mixer retention, 70 cm of tubing, cannula) and nose mouth throat model,

Table I Mean (±SD) Deposition Fraction (DF) at Each Deposition Site as a Percentage of Nominal Dose for the Control (Conventional Sized Aerosol) and EEG Studies ($n \geq 3$ replicates)

	Nebulizer DF (%)	T-connector DF (%)	50 cm tubing DF (%)	20 cm tubing DF (%)	Cannula DF (%)
Control - AS:MN	2.5 ± 0.6	29.6 ± 1.4	13.3 ± 2.3	1.2 ± 0.2	13.4 ± 2.8
Control - AS:NaCl	2.7 ± 0.5	29.1 ± 2.3	13.3 ± 1.8	1.2 ± 0.3	13.2 ± 1.7
EEG - AS:MN	1.4 ± 0.5*	NA	4.7 ± 1.4*	1.0 ± 0.2	0.4 ± 0.04*
EEG - AS:NaCl	1.2 ± 0.3*	NA	2.5 ± 0.7*	0.4 ± 0.1*	0.5 ± 0.2*

* $p < 0.05$ Significant effect on nebulizer, 50 cm tubing, 20 cm tubing, and cannula deposition (One-way ANOVA) compared to respective control formulations (Post hoc Tukey HSD)

together with the dose delivered to the lungs (dose in the impactor) during EEG and control experiments. Note that the delivery device retention for EEG experiments given in Fig. 2 appears higher than the summation of the values given in Table I since the mixer retention, estimated based upon the difference between the nominal dose and the total recovered dose, has been considered in addition to the deposition in the delivery device components, previously listed in Table I. As expected for the conventional sized aerosols, there was significant drug deposition in the delivery device, with approximately 70% of the nominal dose being deposited for both control formulations. In contrast, there were significantly lower device losses ($p<0.0001$) for the submicrometer EEG experiments, with as low as 10.3% deposition being observed for the AS:NaCl formulation. The use of the AS:NaCl formulation in EEG experiments resulted in a significantly lower total device loss compared to the EEG formulation with MN ($p=0.0048$). Importantly for pulmonary delivery, deposition within the NMT model was not significant for the submicrometer EEG formulations (<2%). However, as expected, further significant depositional losses were observed

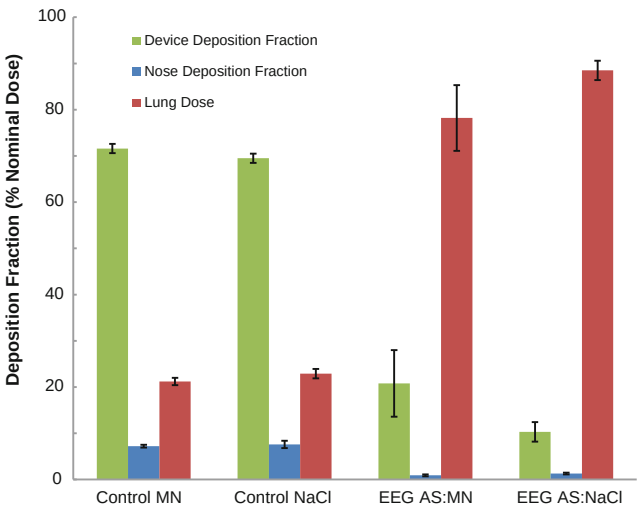

Fig. 2 Mean (SD) % deposition of AS in delivery device (including the estimated mixer retention) and NMT model, together with the lung delivered dose (dose in the impactor) for the control and EEG formulations.

for the conventional sized control aerosols as they were delivered through the NMT model ($p<0.0001$). The type of excipient did not affect the deposition in the NMT significantly ($p=0.7558$). The mean (SD) lung delivered dose for the AS:MN and AS:NaCl EEG submicrometer formulations were 78.2 (7.1) and 88.5 (2.1)%, respectively, which were significantly greater than the doses delivered using the conventionally sized control aerosols ($p<0.0001$). The dose delivered to the lungs was significantly higher using AS:NaCl EEG formulations compared to the AS:MN EEG formulations ($p=0.0052$).

CFD predictions of the regional deposition for the control and EEG aerosols as they enter the cannula and are delivered through the NMT model are shown in Fig. 3. There was good agreement between the deposition fraction predictions and the experimental results. The CFD simulations predicted low deposition in the 20 cm tubing and cannula for the submicrometer EEG formulations, which agreed well with the experimental results. The predictions for NMT deposition for the submicrometer aerosols were higher than the experimental results, but given the overall total low deposition this is expected. The NMT predicted deposition for the control aerosols were observed to agree well with the experimental results.

An essential component to the EEG delivery concept is the condensational growth of the aerosol during inhalation to ensure pulmonary retention of the delivered dose. Figure 4 compares the experimentally determined and CFD predicted aerosol droplet size for the control and submicrometer aerosols at different points in the model. For the conventional delivery cases, the significant depositional losses of the larger droplets reduce the overall MMAD of the aerosol as it is delivered through the NMT model. The final mean (SD) MMADs of the AS:MN and AS:NaCl control aerosols as they exit the NMT model were sized experimentally in the ACI and found to be 0.63 (0.01) and 0.69 (0.03) μm, respectively. These values agreed well with the CFD predicted values (Fig. 4), which predicted that larger particles in control experiments deposit in the nasal cavity and only smaller particles with MMADs of 0.6–0.7 μm reach the trachea. Also shown are the experimentally measured and predicted MMAD of the control aerosols as they exit the cannula prior to entering

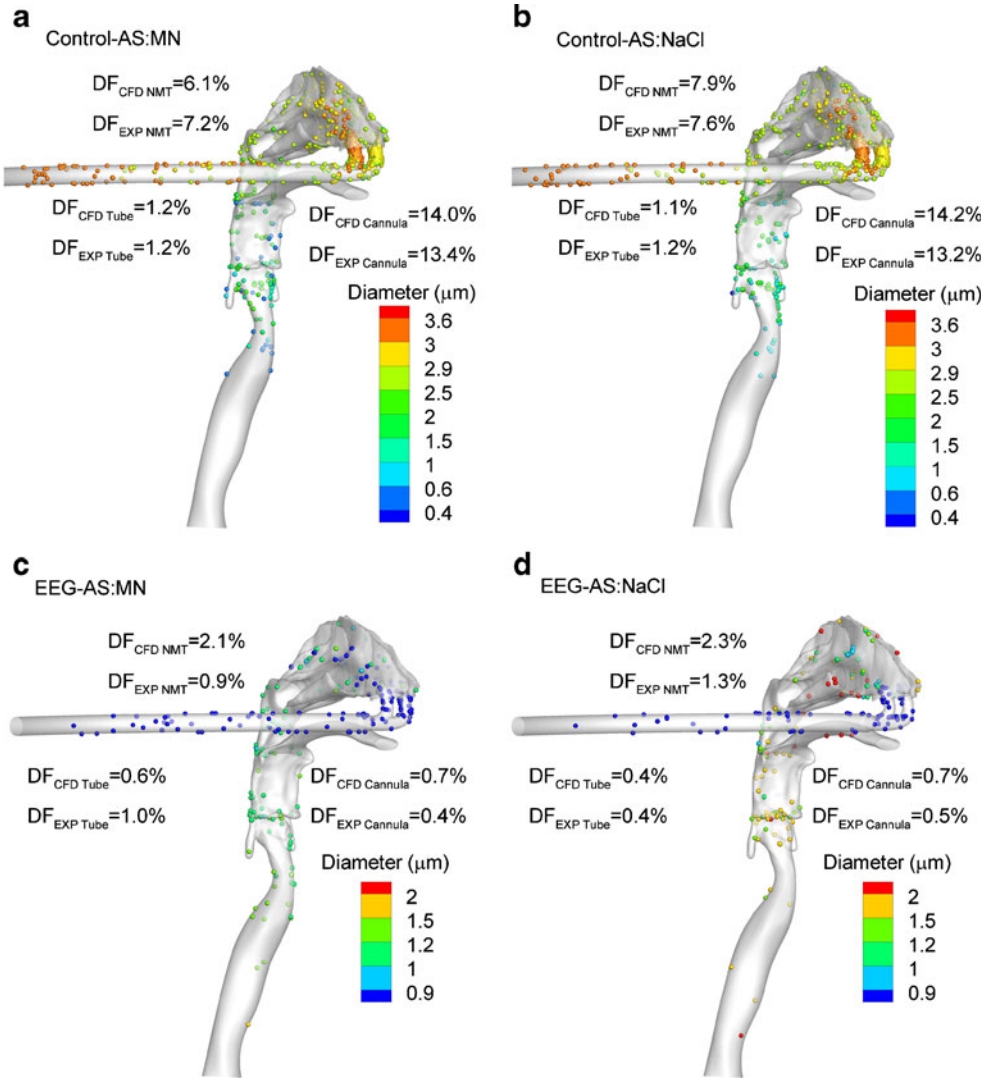

Fig. 3 CFD predictions of regional aerosol deposition colored according to changing particles size in the delivery tube, cannula and NMT model for EEG delivery. Also shown are the predicted (CFD) aerosol drug deposition fractions in these regions compared to the experimental (EXP) results for the control (**a**–**b**) and EEG (**c**–**d**) cases.

the NMT model. Depositional drug losses in the T-connector and ventilator tubing reduced the MMAD from an initial size of 4.8 μm to 2.9 μm. Good agreement between the predicted and measured sizes at the nasal cannula outlet indicate the correct assumption of an initial 3.6 μm aerosol in the CFD control simulations. In contrast with the controls, the MMAD for the AS:MN and AS:NaCl submicrometer EEG aerosols was observed to increase following delivery through the *in vitro* NMT model. The mean (SD) MMADs of the aerosols exiting the NMT were 1.1 (0.1) and 1.55 (0.08) μm, respectively. Again, there was good agreement with the CFD predicted particles sizes, both indicating that the aerosol in EEG experiments increased in size by the time they reach the trachea.

ECG *In Vitro* Deposition

Table II shows the mean (SD) deposition fraction of AS on the delivery device components following aerosolization and delivery to the *in vitro* airway model for the ECG protocol and its control formulations. Drug deposition on the Aeroneb Lab nebulizer was again low (<4%) for each of the ECG formulations, with the drug only formulation showing a significant difference in deposition compared to the control ($p=0.0442$). As with the EEG studies, there was significant drug deposition in the Aeroneb T-connector in the control experiment as the micrometer sized aerosol impacts on this device during mixing with the HFT air. Drug deposition in the 50 cm ventilator tubing that delivers the aerosol from the mixer or T-connector was significantly higher for the conventional sized aerosol compared to the submicrometer ECG aerosols ($p=0.0026$). Deposition within the streamlined ECG cannula was less than 1% of the nominal dose for the submicrometer ECG formulations compared to about 7% for the control experiment. Estimates of mixer drug retention (about 20% of the nominal dose) based upon the difference between the nominal and recovered doses were slightly higher than observed for the EEG experiments; however, this may have been due to some drug loss from the nostril following the introduction of the

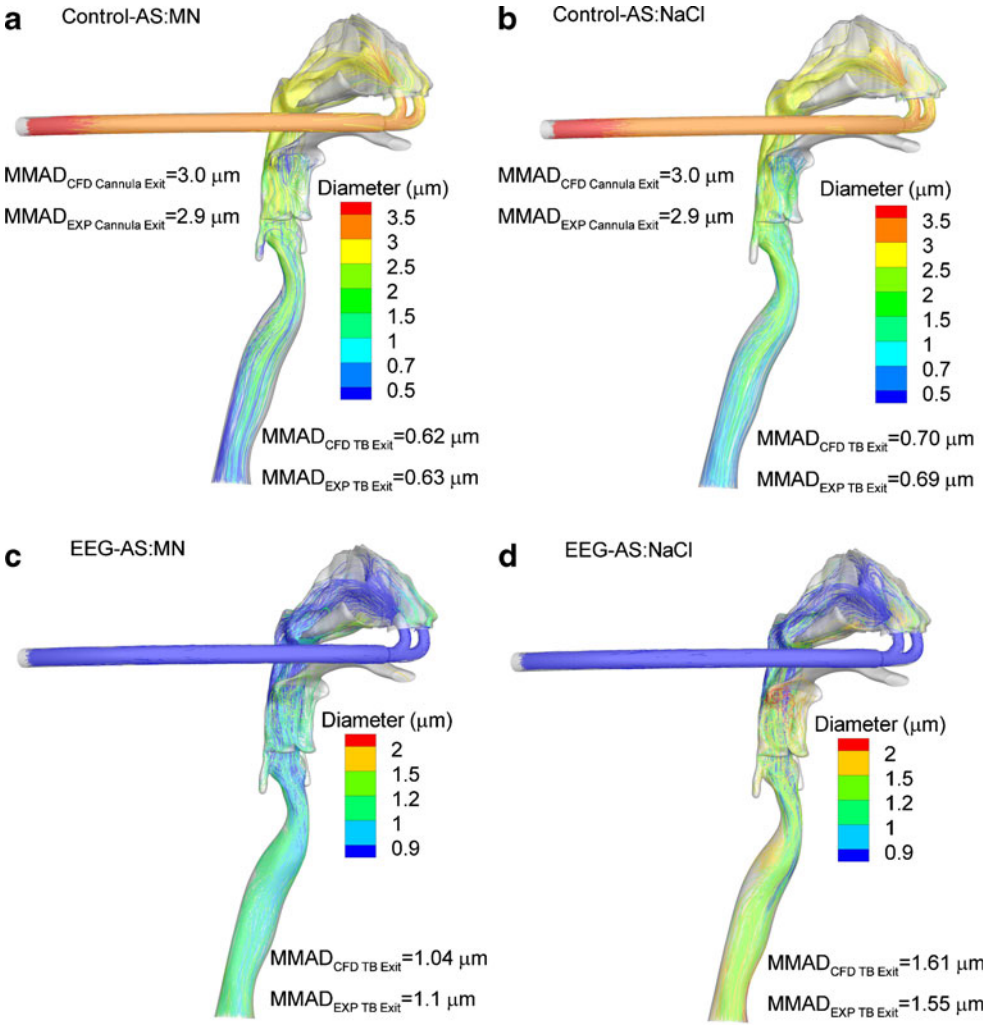

Fig. 4 CFD predictions of aerosol particle trajectories colored according to changing particles size in the delivery tube, cannula and NMT model for EEG delivery. Also shown are predicted aerosol MMADs (CFD) of the aerosol exiting these regions compared to the experimental (EXP) results for the control (**a**–**b**) and EEG (**c**–**d**) cases.

humidified HFT to the model. For all experiments, greater than 80% of the nominal dose was recovered.

Figure 5 shows the % deposition of AS in the delivery device (including the estimated mixer retention in addition to the deposition in the aerosol delivery components given in Table II) and nose mouth throat model, together with the lung delivered dose (dose in the impactor) for the ECG studies. For the conventional sized aerosols, there was about 50% of the drug deposited in the delivery device with a further 20% in the NMT, producing a delivery efficiency available to the lungs of 27.5% of the nominal dose. As observed with the submicrometer EEG formulations, the ECG formulations each showed very low depositional losses in the NMT, with 2% or less of the dose being deposited in the NMT model during steady state inhalation. The mean (SD) lung delivered dose for the AS, AS:MN and AS:NaCl ECG submicrometer formulations were 77.9 (4.4), 74.2 (3.3) and 76.7 (5.5)%, respectively, which was significantly greater than the doses delivered using the conventionally sized control aerosol ($p<0.0001$). The addition of MN or NaCl as a hygroscopic excipient to the drug only formulation did not significantly affect the dose delivered to the lungs ($p=0.4531$ and 0.9678, respectively).

CFD predictions of the regional deposition for the control and ECG aerosols as they enter the cannula and are delivered through the NMT model are shown in Fig. 6. Again, there was good agreement between the deposition fraction predictions and the experimental results for both the control and ECG studies, illustrating that the model is capable of incorporating the additional component of the humidified HFT air delivered along with the aerosol.

Figure 7 shows the condensational growth observed with using the ECG method *vs.* control as droplet trajectories of the aerosols travel through the delivery device and NMT model. For the control case, good agreement is again observed between the experimentally measured and CFD predicted size exiting the nasal cannula and entering the nose. Using a drug only formulation, the mean (SD) MMAD for the aerosol

Table II Mean (±SD) Deposition Fraction (DF) at Each Deposition Site as a Percentage of Nominal Dose for the Control (Conventional Sized Aerosol) and ECG Studies ($n \geq 4$ replicates)

	Nebulizer DF (%)	T-connector DF (%)	50 cm tubing DF (%)	20 cm tubing DF (%)	Cannula DF (%)
Control - AS	3.4 ± 2.6	17.1 ± 1.2	3.7 ± 1.3	0.8 ± 0.3	7.2 ± 2.7
ECG - AS	0.4 ± 0.2*	NA	1.0 ± 0.2*	0.2 ± 0.1*	0.3 ± 0.04*
ECG - AS:MN	3.4 ± 1.5	NA	2.4 ± 1.4	1.2 ± 0.4	0.8 ± 0.3*
ECG - AS:NaCl	0.6 ± 0.2*	NA	2.0 ± 0.6	0.6 ± 0.2	0.4 ± 0.1*

* $p < 0.05$ Significant effect on nebulizer, 50 cm tubing, 20 cm tubing, and cannula deposition (One-way ANOVA) compared to the control formulations (Post hoc Tukey HSD)

exiting the trachea was 1.72 (0.19) μm for ECG delivery with a mean GSD (SD) of 1.62 (0.01). Addition of hygroscopic excipients to the nebulizer formulation produced increased aerosol growth with mean (SD) MMADs of 2.54 (0.12) μm and 2.82 (0.16) μm for the MN and NaCl formulations, respectively. The respective GSDs were 1.62 (0.04) and 1.56 (0.07). As described previously, for the control aerosol, extensive deposition prior to exiting the trachea produces an aerosol with a mean MMAD of 0.72 (0.03) μm with a mean GSD (SD) of 1.65 (0.24). CFD predictions of the final particle sizes were in good agreement with the experimental particles size (Fig. 7) indicating the growth of aerosol in ECG experiments in contrast to the control experiments, where the larger particles deposited in the nasal cavity.

DISCUSSION

Aerosol drug delivery to the lungs during HFT is challenging with conventional sized aerosols due to high drug depositional losses in the delivery device together with additional deposition in the nasal passage. These observations were confirmed in this *in vitro* and CFD study, with losses of approximately 50–70% of the drug dose in the delivery device depending upon the flow rates used. Lower device drug deposition was reported in Tables I and II using a flow rate of 15 LPM (in ECG experiments) compared to 30 LPM (in EEG experiments) presumably due to decreased inertial impaction and turbulent dispersion during transit through the ventilator tubing and cannula. These losses combined with additional deposition in the nasal passage for aerosols with initial MMADs of about 5 μm, which were generated from a conventional mesh nebulizer, resulted in lung delivery efficiencies of between 21.2 – 27.5% of the nominal dose during steady state inhalation. It should be observed that *in vitro* studies often over estimate *in vivo* deposition and that lower delivery efficiency would be expected during transient inhalation rather than the steady state inhalation used in this study. Depositional losses in the T-connector represent the current standard of care when using mesh nebulizers, in which the droplet aerosol exiting the nebulizer deposits by impaction on the T-connector. For EEG and ECG delivery, the T-connector is removed and replaced with a mixer, which is used to generate submicrometer aerosol particles.

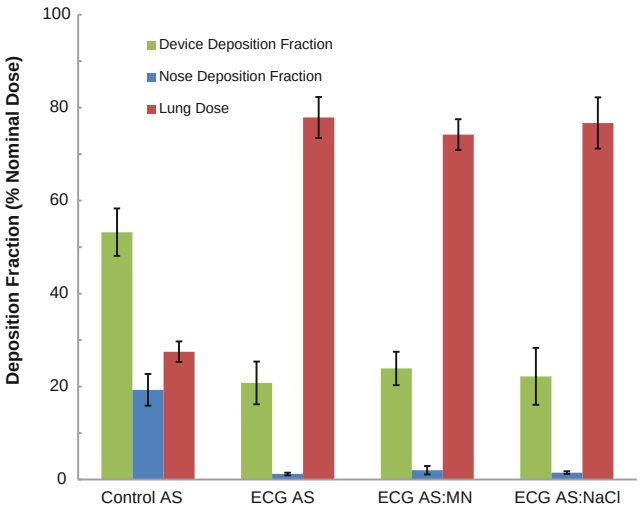

Fig. 5 Mean (SD) % deposition of AS in delivery device (including the estimated mixer retention) and nose mouth throat model, together with the lung delivered dose (dose in the impactor) for the control and ECG formulations.

In contrast with conventional delivery, the *in vitro* data for the EEG submicrometer aerosols demonstrated significantly higher lung delivered doses for both formulations containing MN and NaCl as hygroscopic excipients, respectively ($p < 0.0001$). The ratio of the dose that was delivered to the lungs with EEG conditions compared to their respective controls was almost fourfold higher for each excipient (3.7 fold with MN and 3.9 fold with NaCl). In addition, there was a significantly higher delivery of drug to the lung using the NaCl formulation compared to MN ($p = 0.0052$), which may be related to the increased condensational growth observed for the NaCl formulation. Nasal deposition was around 1% for both EEG formulations suggesting that the submicrometer aerosols were able to penetrate the nasal cavity and enter the trachea without significant depositional losses. The observed significant increases in lung dose are mainly due to reductions in device drug deposition in the ventilator tubing and cannula for the submicrometer aerosol. As a part of the overall decrease

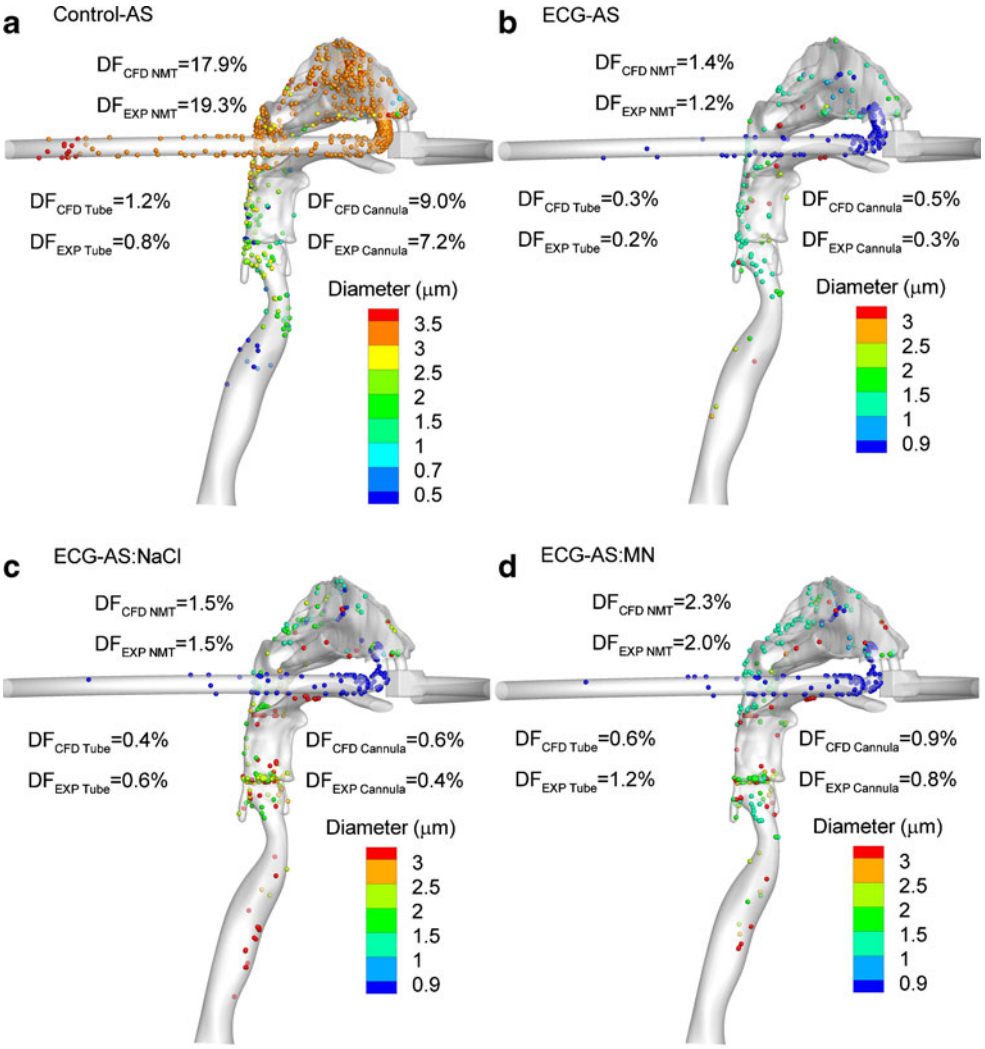

Fig. 6 CFD predictions of regional aerosol deposition colored according to changing particles size in the delivery tube, cannula and NMT model for ECG delivery. Also shown are the predicted (CFD) aerosol drug deposition fractions in these regions compared to the experimental (EXP) results for the control (**a**) and ECG (**b**–**d**) cases.

in the device drug retention, use of the EEG streamlined cannula resulted in nearly zero drug retention for EEG conditions with both excipients (0.4% for the MN and 0.5% for the NaCl formulations).

In order to avoid exhalation of the aerosol, condensational growth of the inhaled EEG droplets is required as the aerosol moves through the respiratory tract. In this study, for the EEG aerosols, it was observed that limited growth had occurred as the drug particles exited the trachea and entered the tracheobronchial region, which based on CFD simulations occurs over a time period of approximately 0.15 s from the point of inhalation at 30 LPM. For the EEG method, condensational growth is dependent upon the hygroscopic excipient present in the formulation and the inherent humidity of the airways. The more hygroscopic sodium chloride formulation was observed to increase in size to 1.5 ± 0.1 μm, compared to 1.1 ± 0.1 μm for the MN formulations at the tracheal exit. Further growth of the aerosol is expected as it penetrates deeper into the airways likely enabling full lung retention. In the tracheobronchial airways, the computational studies of Longest and Hindle (16) and Tian *et al.* (18) predict diameter growth ratios for combination EEG particles up to 5 and higher with final aerosol MMADs as large as 6 μm.

The characteristics of low device deposition, low NMT model deposition and high lung delivered dose were also observed using the ECG delivery mode. For these studies, a line of heated saturated HFT air is delivered using the ECG cannula to one nostril, while the submicrometer aerosol is delivered through a streamlined passageway to the other nostril. Conservative estimates of device drug deposition for the ECG studies were about 20% of the nominal dose, with over 75% of the nominal dose penetrating the NMT and being available for delivery to the lung. The ratio of the dose delivered to the lungs in the ECG case with AS is 2.8 times higher than the lung dose in the control study. This improvement in the lung dose in ECG conditions is again a

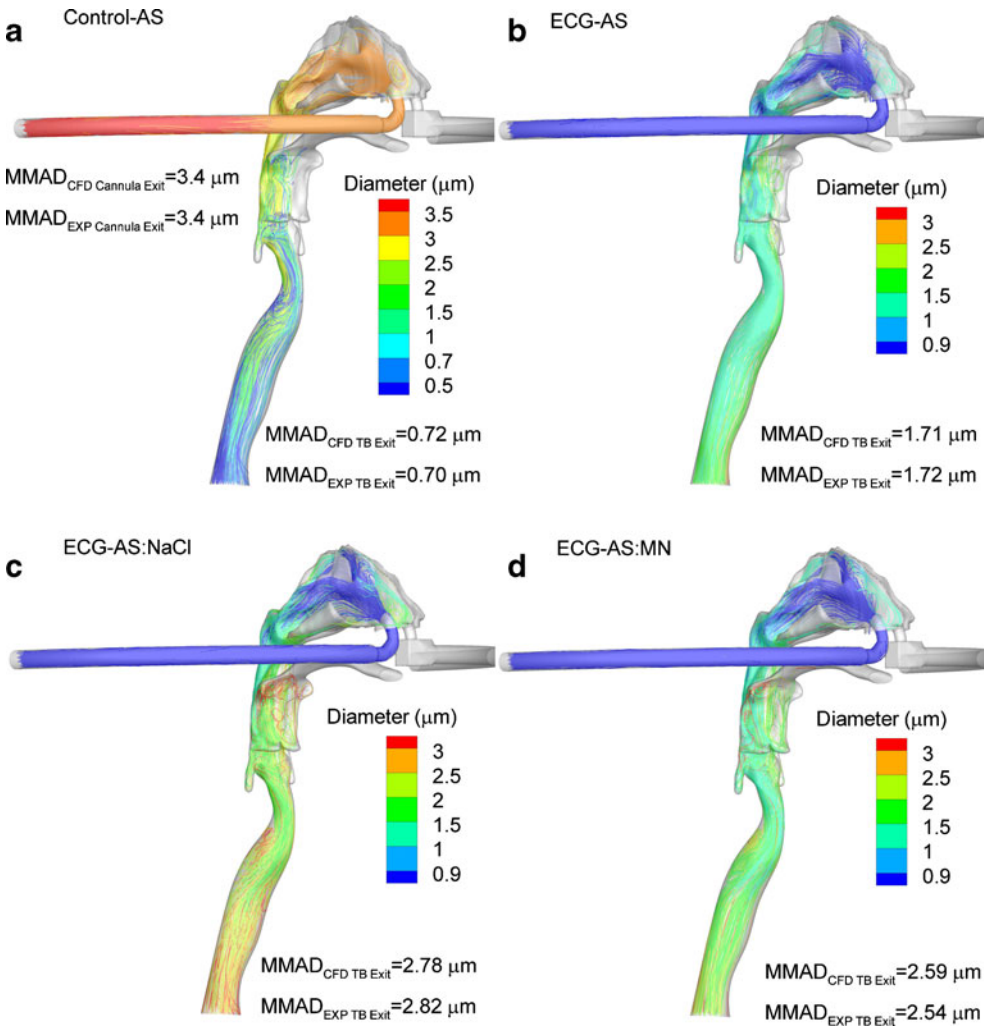

Fig. 7 CFD predictions of aerosol particle trajectories colored according to changing particles size in the delivery tube, cannula and NMT model for ECG delivery. Also shown are predicted aerosol MMADs (CFD) of the aerosol exiting these regions compared to the experimental (EXP) results for the control (**a**) and ECG (**b**–**d**) cases.

result of significantly lower losses in the device components ($p < 0.0001$). Deposition fractions of the submicrometer aerosol within the ventilator tubing and cannula were all less than 4% of the nominal dose for the drug only and hygroscopic excipient containing ECG formulations. As with the EEG method, there were negligible drug deposition losses in the NMT model (1.2-2.0%) using the ECG method, compared to 19.3% for the conventional sized nebulizer aerosol. For the ECG studies, the delivery of supersaturated air, which combines with the aerosol stream after passing beyond the nasal septum, produces a faster rate of condensational aerosol growth compared to the EEG delivery mode. For the three formulations containing AS, AS:MN and AS:NaCl, the mean MMADs at the exit of the trachea were measured as 1.7 μm, 2.5 μm and 2.8 μm, respectively. As a result, additional size increase was observed with the formulations containing the hygroscopic excipients compared to the drug only formulation. The magnitude of growth positively correlates with the hygroscopic parameter; the maximum growth was obtained with the use of NaCl, followed by MN and AS. The increased rate of growth observed with ECG may offer an ability to target deposition sites within the TB airways by controlling the rate of size increase and therefore the deposition site.

Comparing the two delivery modes, both methods successfully reduced the device depositional losses that are commonly observed during HFT. A combination of submicrometer aerosol particles together with a streamlined cannula design were key components in reducing drug losses within the tubing and cannula. This resulted in similar doses being available for deposition in the lungs following passage through the nasal airways. It appears that the EEG technique delivers a slightly higher lung dose compared to the ECG approach; however, the condensation growth was greater for the ECG mode during steady state delivery. A drawback of this present study is the absence of a realistic breathing pattern that is capable of mimicking a normal respiratory cycle. The inclusion of a realistic breath profile will be the subject of a future publication.

Both methods appear suitable for efficient pulmonary drug delivery *via* the nose during HFT. However, as noted previously, growth of aerosol after the NMT is significantly higher ($p<0.0001$) at the tracheal outlet using the ECG technique with hygroscopic excipients compared to EEG (on average 2.8 and 3.1 times growth in ECG, whereas 1.2 and 1.7 times growth in EEG, with MN and NaCl, respectively). Given the success of the EEG and ECG techniques in improving the lung dose, targeted drug delivery to the desired locations in the respiratory system appears to be feasible if it is possible to control the rate and extent of condensational growth. It is envisaged that by controlling the type and concentration of the hygroscopic excipients, in addition to the concentration of the drug in formulations, the fate of inhaled particles in terms of their growth and deposition site can be predicted using the developed CFD models that have been demonstrated in this study. Aerosol deposition and growth predictions using CFD were found to be in close agreement with the *in vitro* experimental data indicating the validity of the models. The relative difference between the regional deposition values in CFD and *in vitro* measurements using both EEG and ECG techniques was mostly <2%. These simulations will be useful for optimizing lung drug delivery by extending the findings in this study to different formulations and experimental conditions.

CONCLUSIONS

A conventional nebulizer (Aeroneb Lab) in combination with an optimized mixer system (13) was successfully used for the generation of submicrometer particles, with an MMAD of ~900 nm, by evaporating the droplets (MMAD ~ 4.5 μm) emitted from the nebulizer. The use of submicrometer particles lowered the delivery device retention and deposition in the extrathoracic airways (*i.e.* NMT model), resulting in significantly higher lung dose compared to the HFT delivery with conventional micrometer-sized aerosols. In order to ensure pulmonary deposition of the aerosol and prevent exhalation, two methods (excipient enhanced growth (EEG) and enhanced condensational growth (ECG)) were used to induce controlled condensational growth of the initially submicrometer particles. The EEG method uses the inherent humidity of the airways in combination with formulation hygroscopic excipients to produce increases in the aerosol particle size. The ECG method increases the particle size of the aerosol by mixing the submicrometer particles (with or without hygroscopic excipients) with supersaturated air that is co-administered to the patient. Computational fluid dynamics (CFD) modeling was performed, in addition to the *in vitro* experiments, which predicted the regional depositions and particle growth in close agreement with the *in vitro* data. Thus, these models can be used to predict the ideal particle size and lung dose of different drugs, used with or without excipients, during nasal inhalation therapies. The use of these condensational growth techniques for the delivery of submicrometer aerosols was found to be a highly efficient method for delivering nasally-administered drugs to the lungs during HFT.

ACKNOWLEDGMENTS AND DISCLOSURES

This study was supported by Award R01 HL107333 from the National Heart, Lung, and Blood Institute. The content is solely the responsibility of the authors and does not necessarily represent the official views of the National Heart, Lung, And Blood Institute or the National Institutes of Health.

REFERENCES

1. Mehta S, Hill NS. Noninvasive ventilation. Am J Respir Crit Care Med. 2001;163:540–77.
2. Dhand R. Aerosol therapy in patients receiving noninvasive positive pressure ventilation. J Aerosol Med and Pulm Drug Deliv. 2012;25(2):63–78.
3. Hess DR. The mask of noninvasive ventilation: principles of design and effects on aerosol delivery. J Aerosol Med. 2007;20:S85–99.
4. Dysart K, Miller TL, Wolfson MR, Shaffer TH. Research in high flow therapy: mechanisms of action. Respir Med. 2009;103:1400–5.
5. Dhand R. Inhalation therapy in invasive and noninvasive mechanical ventilation. Curr Opin Crit Care. 2007;13:27–38.
6. Bhashyam AR, Wolf MT, Marcinkowski AL, Saville A, Thomas K, Carcillo JA, *et al.* Aerosol delivery through nasal cannulas: an *in vitro* study. J Aerosol Med Pulm Drug Deliv. 2008;21:181–7.
7. Fink JB. Aerosol delivery to ventilated infant and pediatric patients. Respir Care. 2004;49:653–65.
8. Parkes SN, Bersten AD. Aerosol kinetics and bronchodilator efficacy during continuous positive airway pressure delivered by face mask. Thorax. 1997;52:171–5.
9. Ari A, Fink JB, Dhand R. Inhalation therapy in patients receiving mechanical ventilation: an update. J Aerosol Med and Pulm Drug Deliv. 2012;25(6):319–32.
10. O'Riordan TG, Greco MJ, Perry RJ, Smaldone GC. Nebulizer function during mechanical ventilation. Am Rev Respir Dis. 1992;145:1117–22.
11. Diot P, Morra L, Smaldone GC. Albuterol delivery in a model of mechanical ventilation. Comparison of metered-dose inhaler and nebulizer efficiency. Am J Respir Crit Care Med. 1995;152(Pt 1):1391–4.
12. Longest PW, Tian G, Hindle M. Improving the lung delivery of nasally administered aerosols during noninvasive ventilation- an application of enhanced condensational growth (ECG). J Aerosol Med Pulm Drug Deliv. 2011;24(2):103–18.
13. Longest PW, Walenga R, Son YJ, Hindle M. High efficiency generation and delivery of aerosols through nasal cannula during noninvasive ventilation. J Aerosol Med Pulm Drug Deliv. 2013. doi:10.1089/jamp.2012.1006.
14. Longest PW, Golshahi L, Hindle M. Improving pharmaceutical aerosol delivery during noninvasive ventilation: effects of streamlined components. Annals Biomed Eng. 2013. doi:10.1007/s10439-013-0759-9.
15. Hindle M, Longest PW. Condensational growth of combination drug-excipient submicrometer particles for targeted high-efficiency pulmonary delivery: evaluation of formulation and delivery device. J Pharm Pharmacol. 2012;64:1254–63.
16. Longest PW, Hindle M. Numerical model to characterize the size increase of combination drug and hygroscopic excipient nanoparticle aerosols. Aerosol Sci Technol. 2011;45:884–99.

17. Longest PW, Hindle M. Condensational growth of combination drug-excipient submicrometer particles: comparison of CFD predictions with experimental results. Pharm Res. 2012;29:707–21.
18. Tian G, Longest PW, Li X, Hindle M. Targeting aerosol deposition to and within the lung airways using excipient enhanced growth. J Aerosol Med Pulm Drug Deliv. 2013. doi:10.1089/jamp.2012.0997.
19. Longest PW, Tian G, Li X, Son YJ, Hindle M. Performance of combination drug and hygroscopic excipient submicrometer particles from a softmist inhaler in a characteristic model of the airways. Annals Biomed Eng. 2012;40(12):2596–610.
20. Hindle M, Longest PW. Evaluation of enhanced condensational growth (ECG) for controlled respiratory drug delivery in a mouth-throat and upper tracheobronchial model. Pharm Res. 2010;27:1800–11.
21. Guilmette RA, Wicks JD, Wolff RK. Morphometry of human nasal airways *in vivo* using magnetic resonance imaging. J Aerosol Med. 1989;2(4):365–77.
22. Kelly JT, Asgharian B, Kimbell JS, Wong B. Particle deposition in human nasal airway replicas manufactured by different methods. Part I: Inertial regime particles. Aerosol Sci Technol. 2004;38:1063–71.
23. Kelly JT, Asgharian B, Kimbell JS, Wong B. Particle deposition in human nasal airway replicas manufactured by different methods. Part II: Ultrafine particles. Aerosol Sci Technol. 2004;38:1072–9.
24. Kimbell JS, Segal RA, Asgharian B, Wong BA, Schroeter JD, Southal JP, *et al.* Characterization of deposition from nasal spray devices using a computational fluid dynamics model of the human nasal passages. J Aerosol Med. 2007;20(1):59–74.
25. Schroeter JD, Garcia GJM, Kimbell JS. Effects of surface smoothness on inertial particle deposition in human nasal models. J Aerosol Sci. 2011;42:52–63.
26. Xi J, Longest PW. Transport and deposition of micro-aerosols in realistic and simplified models of the oral airway. Ann Biomed Eng. 2007;35(4):560–81.
27. Delvadia RR, Longest PW, Hindle M, and Byron PR. *In vitro* tests for aerosol deposition. III: effect of inhaler insertion angel on aerosol deposition. J Aerosol Med Pulm Drug Del. 2013 doi: 10.1089/jamp.2012.0989.
28. Longest PW, Vinchurkar S. Validating CFD predictions of respiratory aerosol deposition: effects of upstream transitions and turbulence. J Biomech. 2007;40:305–16.
29. Xi J, Longest PW, Martonen TB. Effects of the laryngeal jet on nano- and microparticle transport and deposition in an approximate model of the upper tracheobronchial airways. J Appl Physiol. 2008;104:1761–77.
30. Longest PW, Xi J. Condensational growth may contribute to the enhanced deposition of cigarette smoke particles in the upper respiratory tract. Aerosol Sci Technol. 2008;42:579–602.
31. Longest PW, Hindle M, Das Choudhuri S, Byron PR. Numerical simulations of capillary aerosol generation: CFD model development and comparisons with experimental data. Aerosol Sci Technol. 2007;41:952–73.